JPE 2-1-1

An Advanced Three-Phase Active Power Filter with Adaptive Neural Network Based Harmonic Current Detection Scheme

M. Rukonuzzaman* and Mutsuo Nakaoka

Power Electronics System and Control Lab., Yamaguchi University, Japan

ABSTRACT

An advanced active power filter for the compensation of instantaneous harmonic current components in nonlinea current load is presented in this paper. A novel signal processing technique using an adaptive neural network algorithm i applied for the detection of harmonic components generated by three-phase nonlinear current loads and this method car efficiently determine the instantaneous harmonic components in real time. The control strategy of the switching signals tc compensate current harmonics of the three-phase inverter is also discussed and its switching signals are generated with the space voltage vector modulation scheme. The validity of this active filtering processing system to compensate curren harmonics is substantiated on the basis of simulation results.

Key Words: Active Power Filter, Adaptive neural network, Harmonic current compensation

1. Introduction

Current harmonics generated by nonlinear loads such as switching power factor correction converter, converter for variable speed AC motor drives and HVDC systems are causing widespread concern to the power system engineers and have attracted special interest. These harmonics interfere with sensitive electronic devices and cause undesired power losses in electrical equipment. Harmonics cause an array of problems such as equipment overheating, machine vibration, motor failures, capacitor fuse blowing, excessive neutral currents and inaccurate power metering and so forth. To obtain clean power and avoid unwanted power losses, it is a prerequisite to compensate the harmonic current components and active power filters (APFs)[1-4] have been an effective way for

compensating harmonic current components in nonlinea loads.

Active power filters have been widely used due to the recent advancement in power semiconductor devic technology that makes high-speed, high-power switching devices such as power MOSFETs, MCTs, IGBTs, IGCTs IEGTs etc. available for the harmonic curren compensation. Active power filters basically work by detecting the harmonic components from the distortec signals and injecting these harmonic current components with a current of the same magnitude but opposite phase in the power system to eliminate these current harmonics In the active power filter depicted in Fig. 1, the load current, i_L drawn by the nonlinear current source diode rectifier load is sensed by the current transformer (CT) and is sent to the harmonic separator. After detecting the inverse of the total harmonic current component i_c^*, a current controlled three-phase voltage source inverter is used to generate the compensating current i_c and is injected into the utility power source grid. This cancels the harmonic components drawn by the nonlinear load and
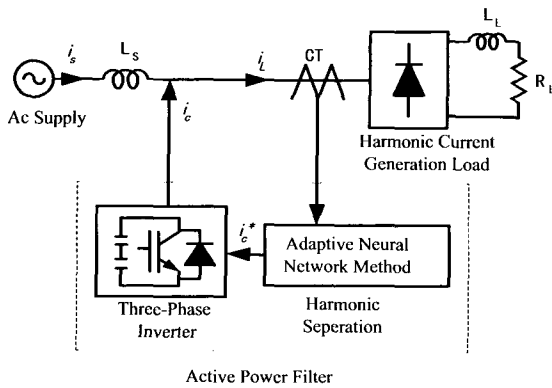
Fig. 1. Schematic representation of active power filter

keeps the utility line current, i_s sinusoidal. A variety of methods are used for instantaneous current harmonics detection in an active power filter such as the FFT (Fast Fourier Transform)[5], instantaneous p-q theory [6], synchronous d-q reference frame theory [7] or by using suitable analog or digital electronic filters [8] separating successive harmonic components. In the FFT technique, the harmonic current determination is delayed by more than two cycles of the operating waveform, one cycle for the data and another cycle for analysis of the data, in order to determine the harmonic components. In the case of harmonic current determination by digital filter, a cascade structure of the bi-quadratic notch filters is necessary which makes the method complicated and its implementation difficult. Other harmonic current detection methods mentioned above have their own downsides and upsides. The disadvantage of synchronous reference frame theory is that it can not compensate for the reactive power. Instantaneous p-q theory can determine the harmonic current components under balanced load conditions only.

In this paper, the harmonic current separation done by the adaptive neural network method [9] is presented which can determine magnitude and phase of fundamental and each of the harmonic current components from which the resultant of harmonic components can be separated. It is noted that harmonic current detection is done in one cycle of the fundamental period. The role of the estimating system is continuously to track the harmonics of the load current and to transfer this information to the compensating devices. The adaptive neural network based signal processing technique is applied for the estimation of harmonic current components in real time in a typical nonlinear three-phase diode bridge rectifier inductive load.

The compensating current generation is achieved with a space vector modulated three-phase current controlled voltage source inverter. The active power filter implementation is verified through computer aided simulations. The DC side voltage of the inverter should be kept controlled for perfect generation of the compensating current and the method to control the DC side voltage of the inverter is also discussed in this paper.

2. Principle of harmonic estimation by adaptive neural network

A three-phase six-pulse diode bridge rectifier generates harmonic currents in the order which is given by

$$n = 6r \pm 1 \tag{1}$$

where, n is the order of the current harmonic and r is an integer $1, 2, 3, ..., R$. In general, the load current in a current source three-phase bridge-rectifier can be expressed as [10]:

$$x(t) = \sum_{l=1,5,7,11...}^{N} X_l \cos(l\omega t - \psi_l) \tag{2}$$

where, X_l is the magnitude and ψ_l is the phase of the lth harmonic component ($l=1, 5, 7, 11, ..., N$) and ω is the fundamental angular frequency.

Equation (2) can be written as,

$$x(t) = \sum_{l=1,5,7,11...}^{N} (A_l \cos l\omega t + B_l \sin l\omega t) \tag{3}$$

where, $A_l = X_l \cos \psi_l$ and $B_l = X_l \sin \psi_l$. Magnitude and phase of each harmonic can be determined as follows:

$$X_l = \sqrt{A_l^2 + B_l^2} \tag{4}$$

$$\psi_l = \arctan\left(\frac{B_l}{A_l}\right) \tag{5}$$

The eqn. (3) can be rewritten as:

$$x(t) = A_1 \cos \omega t + B_1 \sin \omega t$$
$$+ \sum_{j=1}^{R} \left[\begin{array}{c} A(6j \pm 1) \cos(6j \pm 1)\omega t \\ +B(6j \pm 1) \sin(6j \pm 1)\omega t \end{array} \right] \tag{6}$$

where, $j=1, 2, 3, ..., R$ and $N=6R\pm1$.

In generic neural network, there are two main process involved- training and testing. In the training process, the network is trained with suitable inputs and output patterns so that the outputs of the neural network approximate the target values for various input training patterns in the training set. In the testing process, the performance of the network is verified by using the input data outside the training set. However, in this paper, instead of training the network, we use the basic principle of neural networks, that is the objective function, to determine adaptively the fundamental and the harmonic components of the distorted load current.

In an adaptive estimation of harmonic current components by neural networks, the load current is sampled uniformly and one sample is taken at a time. The sampled values are used to determine the magnitude and phase of the fundamental and harmonic current components through the adaptive neural circuit. The objective function of the neural network is used to minimize the error that is the difference between the measured samples of the load current d_k at time t_k (as shown in Fig. 2 and output of the neural circuit generated in an adaptive way. In this method, one sample is taken and the corresponding harmonic and fundamental components are determined through the neural circuit and then sent back. These values are used for calculation when the next sample is taken. In this fashion, the harmonic current components can be determined within one time period of the fundamental component. The instantaneous mean squared error at the kth iteration is then described on the basis of the objective function [11]:

$$\xi_k = 0.5[x(t_k)-d_k]^2 \qquad (7)$$

or

$$\xi_k = 0.5\left(A_1 \cos\omega t_k + B_1 \sin\omega t_k + \sum_{j=1}^{R}\left[A_{(6j\pm1)}\cos(6j\pm1)\omega t_k + B_{(6j\pm1)}\sin(6j\pm1)\omega t_k\right] - d_k\right)^2 \qquad (8)$$

Since ω is known and the time instant t_k is fixed, the terms $cos(6j\pm1)\omega t_k$ and $sin(6j\pm1)\omega t_k$ form the coefficients
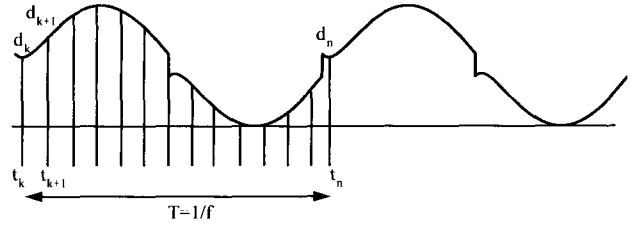

Fig. 2. Sampling of the distorted load current for harmon current determination

of unknown variables $A_{(6j\pm1)}$ and $B_{(6j\pm1)}$ and can be denote by vector notation at the kth iteration as:

$$X_k = [A_1, B_1, A_5, B_5, A_7, B_7, ..., A_N, B_N]^t \qquad (9$$

And the input pattern denoted by Y_k is given by:

$$Y_k = \begin{bmatrix} \cos\omega t_k \\ \sin\omega t_k \\ \cos5\omega t_k \\ \sin5\omega t_k \\ \cos7\omega t_k \\ \sin7\omega t_k \\ \cdot \\ \cdot \\ \cdot \\ \cos N\omega t_k \\ \sin N\omega t_k \end{bmatrix} \qquad (1C$$

Eq. (7) can be represented in quadratic form by [12

$$\xi_k = 0.5\left(d_k^2 - 2d_k Y_k^t X_k + X_k^t Y_k Y_k^t X_k\right) \qquad (11$$

According to the neural network principle [13, 14], th optimum point of the objective function eq. (7 corresponds to the steady state solution of the differentia equation;

$$\frac{dX_k}{dt} = -K\Delta\xi_k \qquad (12$$

where, K denotes the constant of integration and

$$\Delta\xi_k = \left[\frac{\delta\xi_k}{\delta A_1}\frac{\delta\xi_k}{\delta B_1}\frac{\delta\xi_k}{\delta A_5}\frac{\delta\xi_k}{\delta B_5}......\frac{\delta\xi_k}{\delta A_N}\frac{\delta\xi_k}{\delta B_N}\right]^t \qquad (13$$

$$\frac{\delta \xi_k}{\delta A_l} = \begin{bmatrix} A_1 \cos \omega t_k + B_1 \sin \omega t_k \\ + \sum_{j=1}^{R} \begin{bmatrix} A_{(6j\pm1)} \cos(6j\pm1)\omega t_k \\ + B_{(6j\pm1)} \sin(6j\pm1)\omega t_k \end{bmatrix} - d_k \end{bmatrix} \cos(l\omega t_k)$$

(14)

$$\frac{\delta \xi_k}{\delta B_l} = \begin{bmatrix} A_1 \cos \omega t_k + B_1 \sin \omega t_k \\ + \sum_{j=1}^{R} \begin{bmatrix} A_{(6j\pm1)} \cos(6j\pm1)\omega t_k \\ + B_{(6j\pm1)} \sin(6j\pm1)\omega t_k \end{bmatrix} - d_k \end{bmatrix} \sin(l\omega t_k)$$

(15)

From Eqs. (9), (12) and (14)

$$A_l = -K \int \begin{bmatrix} A_1 \cos \omega t_k + B_1 \sin \omega t_k \\ + \sum_{j=1}^{R} \begin{bmatrix} A(6j\pm1)\cos(6j\pm1)\omega t_k \\ + B(6j\pm1)\sin(6j\pm1)\omega t_k \end{bmatrix} - d_k \end{bmatrix} \cos(l\omega t_k) dt$$

(16)

From Eqs. (9), (12) and (15)

$$B_l = -K \int \begin{bmatrix} A_1 \cos \omega t_k + B_1 \sin \omega t_k \\ + \sum_{j=1}^{R} \begin{bmatrix} A(6j\pm1)\cos(6j\pm1)\omega t_k \\ + B(6j\pm1)\sin(6j\pm1)\omega_k t \end{bmatrix} - d_k \end{bmatrix} \sin(l\omega t_k) dt$$

(17)

The neural circuit implementation for the determination of the values of A_l and B_l ($l=1, 5, 7, 11,13,\ldots\ldots, N$) according to eqns. (16) and (17) is represented in Fig. 3. Then, the magnitude and the phase of the fundamental and harmonic current components can be obtained by applying eqn. (4) and (5).

In short, the adaptive neural network methods of harmonic detection can be summarized as:

a. Setting the value of constant of integration, K

b. Setting all A_l and B_l values to zero

c. Sampling of the load current uniformly and getting sample value d_k at time t_k

d. Determination of the values of A_l and B_l according to Eqs. (16) and (17).

e. Taking the next sampled value
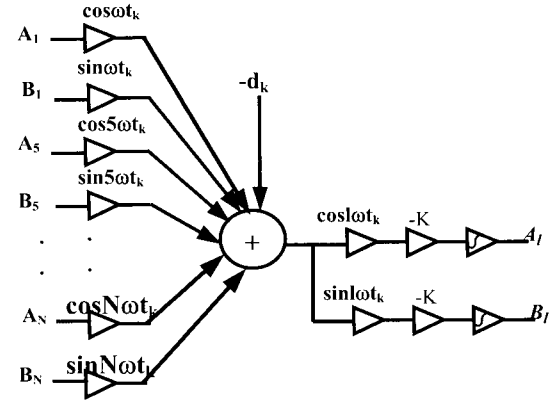
f. Continuation of steps d and e for one complete cycle

Fig. 3. Neural circuit for adaptive estimation of A_l and B_l (l=1, 5 7, 11,13,....., N).

3. Complete APF operation

3.1 System Description

The complete active power filter operation is illustrated in Fig. 4 with the DC side voltage control of the 3-phase current controlled voltage source type inverter and the generation of compensating current with space voltage vector modulation technique. In Fig. 4, the adaptive neural network method determines the fundamental components (i_{af}, i_{bf}, and i_{cf}) of the nonlinear load currents (i_a, i_b, and i_c) and the fundamental components are subtracted from the load currents to get the harmonic components (i_{ah}, i_{bh}, and i_{ch}). The total harmonic current present in the load is computed by subtracting the fundamental component from the load current and not from the summation of the harmonic current components. The reason for this is that not all harmonics present in the load current are computed by the adaptive neural network method and only up to 25th harmonic current components are computed by this method. The harmonic current components are converted to the dq axis components (i_{dh}, and i_{qh}) through abc-dq phase transformation. And these d-q axis components (with modified direct axis component for keeping the inverter DC side voltage constant) together with the values of the dq transformed supply voltages and dq transformed inverter phase voltages are applied for the calculation of the command voltage vector digitally. From these command voltages through Space vector modulation technique, the gating signals of the three-phase voltage source inverter for generating compensating currents are determined and applied to the inverter through its gate drive circuit.
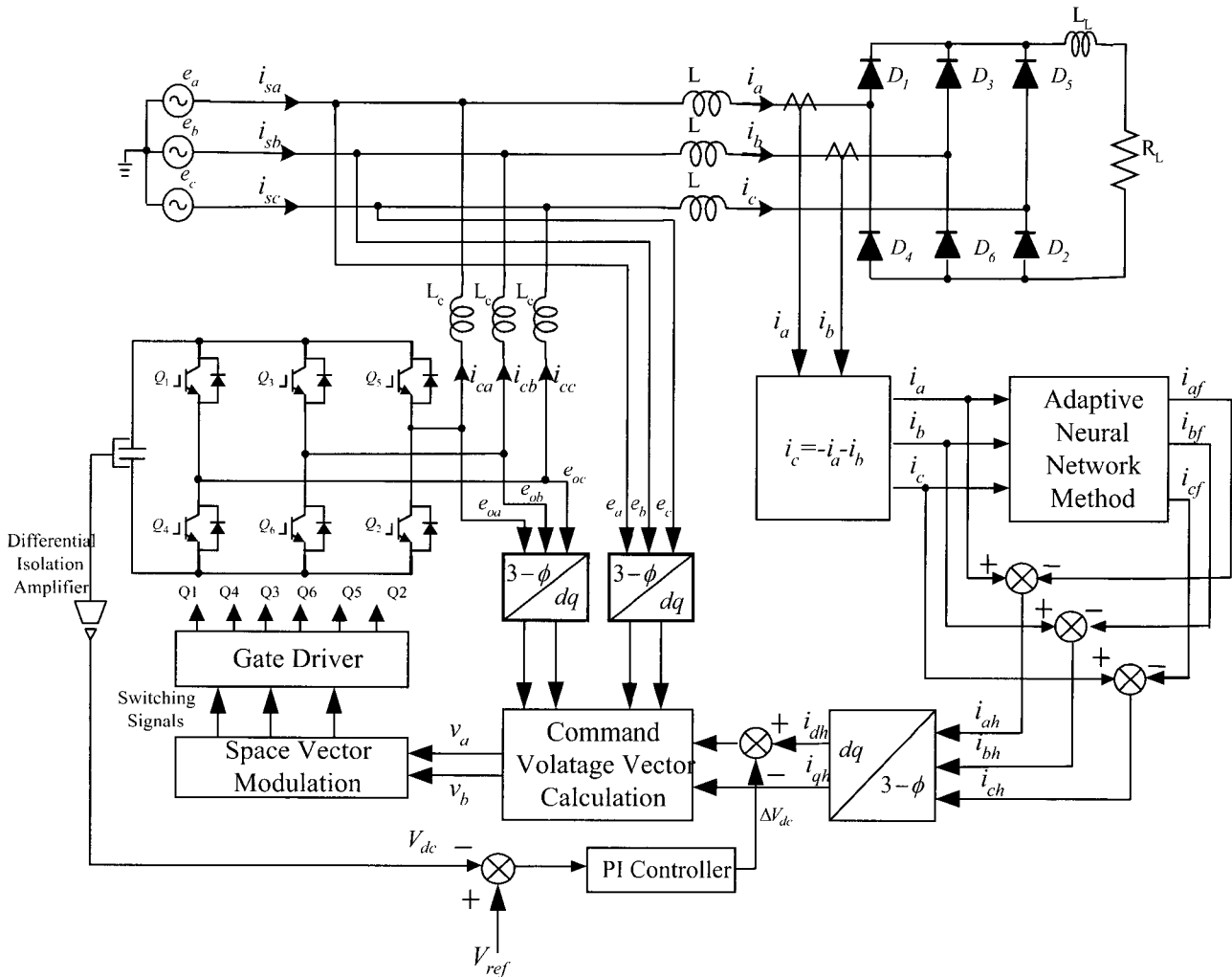
Fig. 4. Control circuit for reference voltage with harmonic detection process.

3.2 DC side voltage control

The DC side voltage of the space voltage vector modulated voltage source inverter should be controlled and kept at a constant value to maintain the normal operation of the inverter. Because there is an energy loss due to conduction and switching power losses associated with the diodes and IGBTs of the inverter in APF which tend to reduce the value of Vdc across capacitor Cdc. A feedback voltage control circuit needs to be incorporated into the inverter for this reason. The difference between the reference value, Vref and the feedback value, Vdc first passes a PI (Proportional Integral) controller and the output of the PI controller is subtracted from the direct axis value of the harmonic current components. Therefore, additional fundamental components are added to the load

harmonic currents. Eventually when the three-phase voltage source inverter is producing the required harmonic current, additional fundamental current component is provided. The fundamental current interacts with the fundamental source current and can then control the energy flow of the inverter to maintain the value of the DC side voltage of inverter constant.

3.3 Generation of space vector modulation (SVM) signal

The switching signals for the voltage source inverter are generated by applying space voltage vector modulation scheme to produce the total compensating currents. The switching signals are used to control the gating of the voltage-fed three-phase inverter that in turn produces a
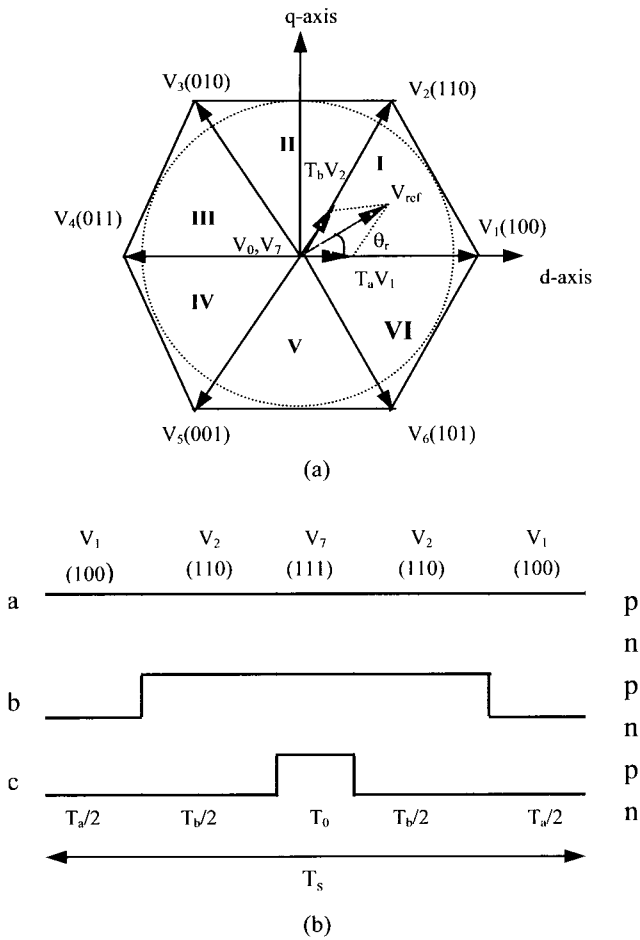
q-axis

Fig. 5. (a) Voltage space vectors in a complex d-q plane; (b) Gating signals during one sampling period in sector I.

three-phase voltage output. The voltage is applied across the injection inductor, which through the use of differential equation determines the current flowing through the inductor.

Any set of three-phase quantities that add up to zero in the a-b-c coordinate $\left([x]_{abc}=[x_a x_b x_c]^T\right)$ can be represented by two-dimensional complex space[15]. The resulting vector in complex notation $\left(X=[x]_{dq}\right)$ is presented by:

$$\begin{bmatrix} x_d \\ x_q \end{bmatrix} = \begin{bmatrix} 1 & -1/2 & -1/2 \\ 0 & \sqrt{3}/2 & -\sqrt{3}/2 \end{bmatrix} \begin{bmatrix} x_a \\ x_b \\ x_c \end{bmatrix} \qquad (18)$$

The switching states in a three-phase voltage source type inverter results in six non-zero space voltage vectors

(V_k, k=1, 2,..., 6) forming an hexagon centered at the origin of the d-q coordinate plane, and the remaining two zero voltage space vectors (V_0, V_7) are located at the origin of the d-q plane. The eight space voltage vectors and the corresponding hexagon are illustrated in Fig. 5 (a).

When the reference vector is in region I, two non-zero vectors V_1, V_2 and either V_0 or V_7 are applied. The duty cycles T_a and T_b of two space vectors and T_0 of the zero vector are specified by[16],

$$T_a = M \sin(60 - \theta_r)T \qquad (19)$$

$$T_b = M \sin(\theta_r)T \qquad (20)$$

$$T_0 = T - T_a - T_b \qquad (21)$$

where, T is the cycle period, M is the modulation index and θ_r is the angle between reference vector and the nearest clockwise state vector. The voltage vector distribution used in this paper is by far the most prevalent because of its harmonic advantage and low switching loss production and is depicted in Fig. 5(b) during one sampling period in the sector I.

4. Simulation Results and Discussions

The harmonic current compensation by the active power filtering is implemented in a three-phase power system with the utility power supply voltage of 200 V and current source type three-phase diode-bridge rectifier with inductive load as the harmonic current compensation object. The adaptive neural network circuit is implemented using a programming language but in practical case it can be implemented through digital signal processing.

Since the method for the fundamental and harmonic current component detection is adaptive and sampled values are used, the sampling frequency is an important factor in determining the harmonic current components. As mentioned earlier, the harmonic current components can be determined in one fundamental period and that is illustrated in Fig. 6. This figure shows the adaptive determination of magnitude of the fundamental and the 7th order harmonic current components.
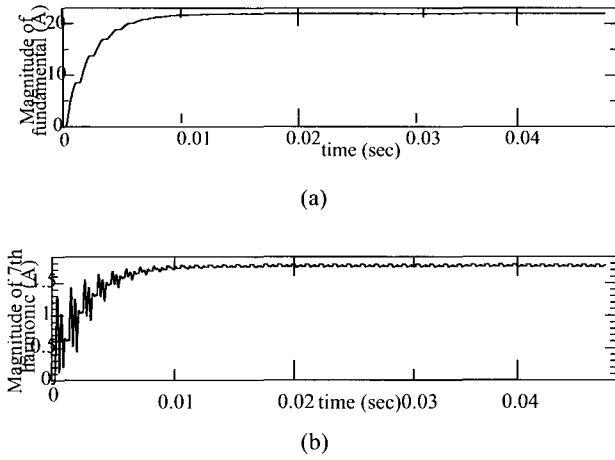
(a)

(b)

'ig. 6. Adaptive estimation of (a) the magnitude and (b) 7th iarmonic component of the load current in phase a. when the ampling frequency is 9 kHz.

(a)

(b)

Fig. 7. Adaptive estimation of (a) the magnitude and (b) 7th harmonic component of the load current in phase a. when the sampling frequency is 6 kHz.

The values of the fundamental and the harmonic current components are constant after one cycle which ubstantiates our supposition that harmonic currents can ie determined in one cycle of the fundamental period and vhatever the initial values of the harmonic current omponents are assigned, the adaptive method can letermine the magnitude and the phase of harmonic urrent components as well as the total compensating urrent accurately and in an adaptive fashion. In this case, he sampling frequency used was 9 kHz and the value of he constant of integration, K was 0.0125 in the simulation. he sampling frequency that is the total number of amples, plays an important role in determining the iarmonic current components in a nonlinear load and this ffect is shown in Fig. 7 where the sampling frequency is ı kHz. In this case, the 7th harmonic component magnitude luctuate slightly even after one cycle period and the Total larmonic Distortion (THD) after harmonic compensation n the load current is approximately one percent more than vhen the frequency is 9 kHz. Sampling frequencies are aried to observe the performance of adaptive neural ietwork on determining the harmonic components and the ampling frequency that provides minimum THD is hosen in this paper. Therefore, the sampling frequency hould be chosen such that it can perfectly estimate the ompensating current.

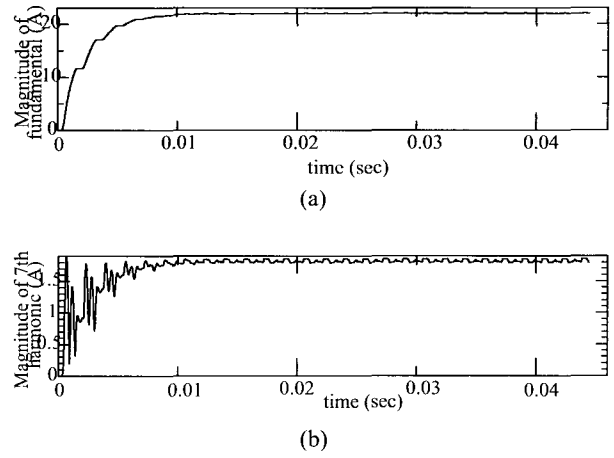The design specifications and the circuit parameters sed in the simulation are indicated in Table 1.

Table 1. Design specifications and circuit parameters.

Sampling frequency	9 kHz
Switching frequency	12 kHz
Fundamental frequency	60 Hz
AC supply voltage	200 V [RMS]
Inverter DC voltage, V_{dc}	350 V
Rectifier load inductance, L_L	15 μH
Rectifier load resistance, R_L	13 Ω
Rectifier side inductance, L	1.84 mH
Inverter side injection inductance, L_c	0.01 H
Partial gain of PI controller, K_P	4.9
Integral gain of PI controller, K_I	0.9
Inverter DC side capacitance, C_{dc}	5000 μF

The distorted load current waveform in phase a is shown in Fig. 8(b). The compensating current waveform estimated by the proposed adaptive neural network in phase a is illustrated in Fig. 8(c) and demonstrates that the adaptive neural network method can exactly keep track of the harmonic current components. The compensating current generated by three-phase current controlled voltage source inverter is also illustrated in Fig. 8(d). The utility power source current after the harmonic compensation is illustrated in Fig. 8(e). From the waveform of the source current after the compensation it can be stated that the source current is sinusoidal and

(a)
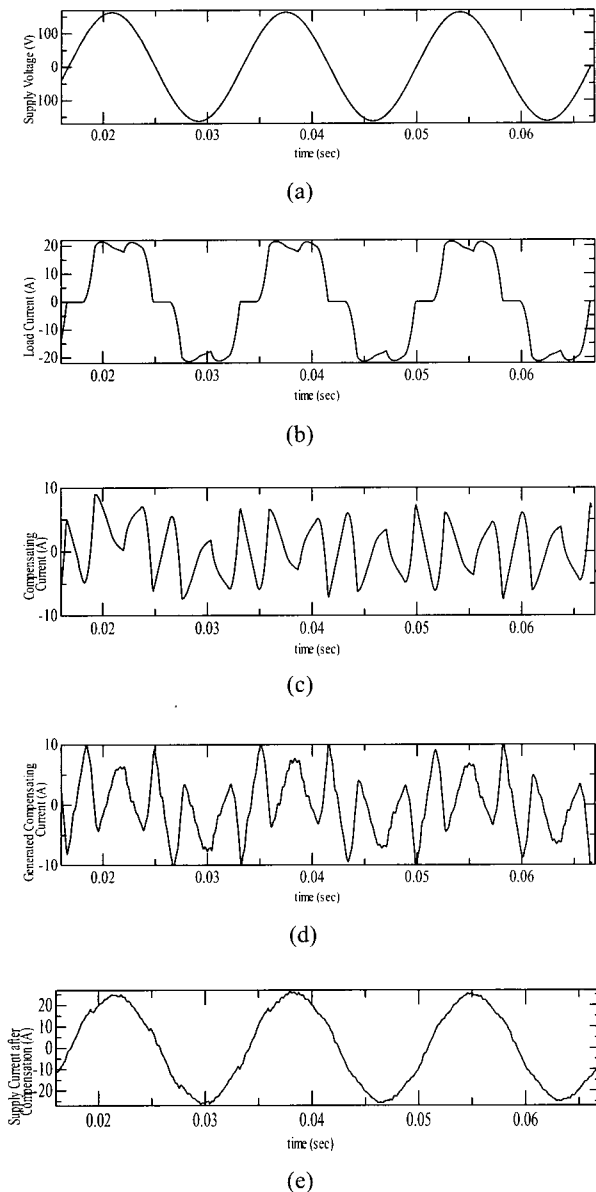

(b)

(c)

(d)

(e)

Fig. 8. Operating waveforms of (a) Supply voltage, (b) Load current and (c) Compensating current, (d) Generated compensating current and (e) supply current after harmonic compensation in phase a.

instantaneous harmonic currents are compensated quite accurately. The THD (Total Harmonic Distortion) is also computed in load current as well as in supply current. The THD is 23.34% before harmonic compensation in load current and 5.64% in supply current after harmonic current compensation that is within the specified limit of the harmonic standard regulated by IEEE. The DC side voltage of the inverter is represented in Fig. 9 and is

almost constant with a little deviation. This is due to the fact that extra dc component is required to overcome the losses associated with APF switches.

The average switching frequency of the inverter is selected as 12 kHz and thus theoretically it can compensate up to 200th harmonic current components. A delay of 2 μs is added in the switching signal to ensure that both the active power switches in each inverter bridge leg are not switched on simultaneously.
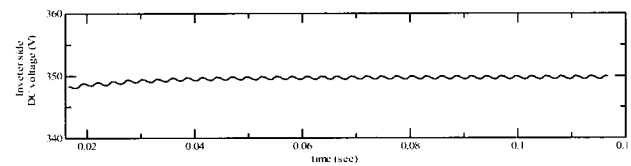

Fig. 9. Inverter side DC voltage across C_{dc}

5. Transient Response of APF

In order to obtain the best performance from the APF the system is tested in the steady state as well as in the transient conditions. For this reason, the parameters of the nonlinear load are changed from one value to another. Fig 10 illustrates the transient response of the nonlinear load when the load is changed to the value of R=26.5 Ω and L=4.5mH and from this figure it is seen that the supply current changes with the change in load current. The transition of the load current at time 0.0667 sec is smooth between two consecutive time instants and the adaptive neural network method can effectively keep track of this change in the load current as can be seen from the waveform of the compensating current shown in Fig 10(b). The generation of compensating current by the SVM controlled three-phase voltage source inverter i shown in Fig. 10(c) and it illustrates the performance o the voltage source inverter. The supply current as shown in Fig. 10(d) is also sinusoidal after the change in load current that means that the active power filter system' performance is up to the mark in transient condition. But there is one drawback of this method with the transient response, that is, we have to wait for one fundamental cycle as the adaptive neural network method requires one cycle of the fundamental period to determine the harmonic current.
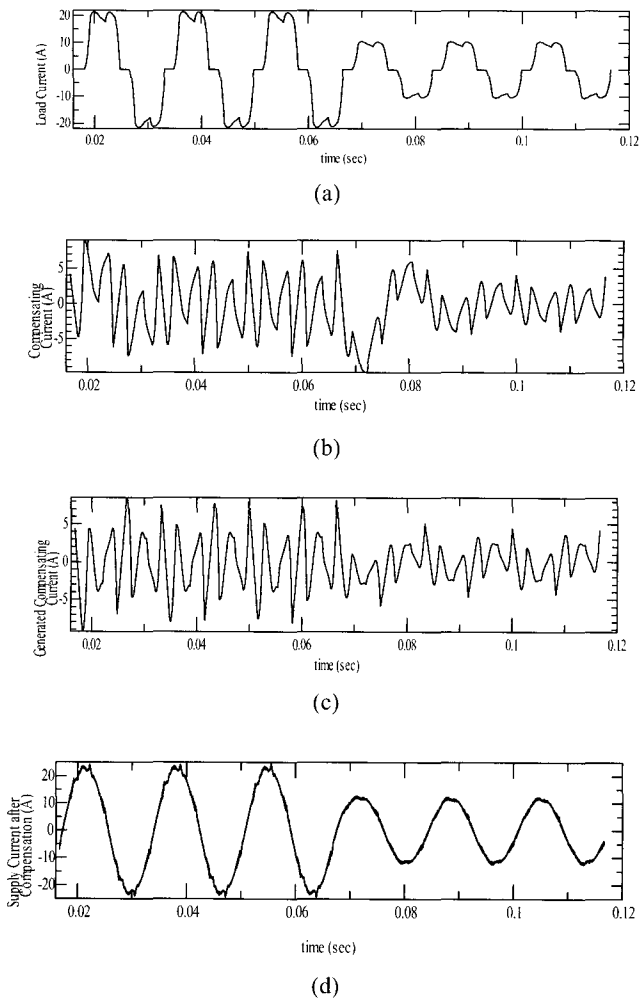
6. Conclusions

The advanced APF with adaptive neural networ scheme presented in this paper for the compensation c harmonic current components in non-linear load we effective for harmonic isolation and keeping the utilit supply line current sinusoidal. The method used to contre the DC side voltage of the three-phase inverter wa capable of maintaining the voltage constant. The adaptiv neural network current detecting scheme could determin the current harmonic components effectively an accurately and could compensate the harmonic currents i real time. The validity of this parallel active filterin; technique in order to compensate current harmoni components was proved on the basis of simulation results.

Because of the magnitude and phase determination b; this adaptive neural network method, it can also b implemented for power factor correction in nonlinear load

Fig. 10. Operating waveforms of (a) Load current (b) Compensating current, (c) Generated compensating current and (d) supply current after harmonic compensation during steady state and transient conditions.
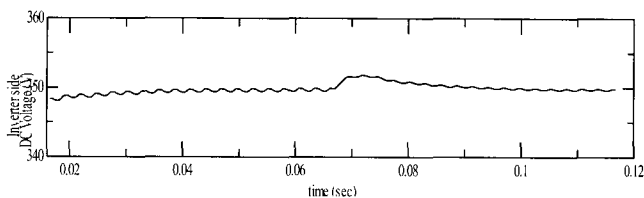
Fig. 11. DC voltage across C_{dc} during steady-state and transient condition.

The DC side voltage waveform across the capacitor of the inverter in the transient as well as steady state condition is also shown in Fig. 11 and is fairly constant around 350 V.

References

[1] D. M. E. Ingram and S. D. Round, "A fully digita hysteresis current controller for an active power filter", In. Journal of Electronics, Vol. 86, No. 10, pp. 1217~1232.

[2] R. P. Stratford, "Analysis and control of harmonic curren in systems with static power converters", IEEE Trans. or Ind. Appl., Vol. IA-17, No. 1, Jan./feb. 1981.

[3] H. Akagi, A. Nabae, and S. Atoh, "Control strategy o active power filters using Voltage-Source PWN Converters", IEEE Trans on Ind. Appl., Vol. 22, No. 3, pp 460, 1986.

[4] H. Sasaki, and T. Machida, "A new method to eliminate AC harmonic currents by magnetic flux compensation - considerations on basic design", IEEE Trans. on Powei Apparatus and System. PAS-90, pp. 2009~2019, 1971.

[5] A. Ametani, "Harmonic reduction in thyristor converter; by harmonic current injection", IEEE Trans. Power. App Syst., Vol. 95, pp. 441~449, Mar./Apr. 1976.

[6] H. Akagi, Y. Kanazawa, and A. Nabae, "Instantaneou; reactive power compensators comprising switching devices without energy storage components", IEEE Trans. Ind. App., Vol. IA-20, pp. 625~630, May/June 1984.

[7] S. Bhattacharya, and D. M. Divan, "Hybrid serie; active/parallel passive power line conditioner with controlled harmonic injection", U.S. Patent 5 465 203 Nov. 1995.

[8] T. Kwan, and K. Martin, "Adaptive detection and enhancement of multiple sinusoids using a cascade of IIR filters", *IEEE Trans*. CAS-36, pp. 936~947, 1989.

[9] M. Rukonuzzaman and M. Nakaoka, "An advanced active power filter with adaptive neural network based harmonic detection scheme", *Proceedings of IEEE-PESC.*, Vol. 3, pp. 1602~1607, 2001

[10] R. Yacamini, "Power system harmonics- part1 harmonic sources", *Power Engineering Journal*, pp. 193~198, August 1994.

[11] S. Osowski, "Neural network for estimation of harmonic components in a power system", *IEE proceedings-C*, Vol. 139, No. 2, March 1992.

[12] B. Widrow, and S. Stearns, *Adaptive signal processing*, Prentice Hall, Englewood Cliffs, New York, 1985.

[13] M. Kennedy, and L. O. Chua, "Neural networks for nonlinear programming", *IEEE Trans.*, CAS-35, pp. 554~562, 1988.

[14] D. W. Tank, and J. J. Hopfield, "Simple neural optimization networks", *IEEE Trans.*, CAS-33, pp. 533~541, 1986.

[15] J. Holtz, "Pulsewidth modulation – A survey", *IEEE Trans. on Industrial Electronics*, Vol. 39, No. 5, pp. 410~420, 1999.

[16] A. Bakhshai, J. Espinoza, G. Joos, and H. Jin, "A combined artificial and DSP approach to the implementation of space vector modulation techniques", *Proceedings of IEEE IAS Annual Meeting*, Vol. 2, pp. 934~940, 1996.
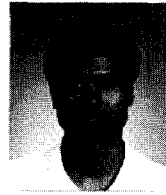
M. Rukonuzzaman was born in Jamalpur, Bangladesh in 1971. He received his B. Sc. in Electrical and Electronics Engineering from Bangladesh University of Engineering and Technology (BUET) in 1995 and Master of Engineering from University of Technology, Malaysia in 1998. He is currently doing research in Division of Electrical Systems Engineering, the Graduate School of Engineering and Science, Yamaguchi University, Yamaguchi, Japan towards his Ph. D. degree. His research interests include active power filtering, application of artificial intelligence in power electronics and soft switching technology. He is a student member of IEEE, USA and IEEJ, Japan.

Mutsuo Nakaoka was born in Hiroshima, Japan. He received his Ph. D degree in Electrical Engineering from Osaka University, Osaka, Japan in 1981. He joined in the Electrical and Electronics Engineering Department, Kobe University Kobe, Japan in 1981. Since 1995, he has been a professor in the Electrical and Electronics Engineering Department, the Graduate School of Engineering and Science, Yamaguchi University, Yamaguchi, Japan. His research interests include state-of-the-art power electronics circuits and systems engineering. Dr. Nakaoka is a member of the Institute of Electrical Engineers of Japan, Institute of Electronics, Information, and Communication Engineers of Japan, Institute of Illumination Engineering of Japan, the Institute of Installation Engineers of Japan and Senior Member of IEEE, USA.